Radiation Effects & Defects in Solids
Vol. 166, No. 4, April 2011, 313–322

Taylor & Francis
Taylor & Francis Group

Downloaded By: [CSIR eJournals Consortium] At: 05:32 27 March 2011

DLTS and *in situ* C–V analysis of trap parameters in swift 50 MeV Li^{3+} ion-irradiated $Ni/SiO_2/Si$ MOS capacitors

N. Shashank[a]*, Vikram Singh[b], Sanjeev K. Gupta[b], K.V. Madhu[c], J. Akhtar[b] and R. Damle[c]

[a]*Department of Electronics, Kuvempu University, Shankaraghatta-577451, India;* [b]*Sensors and Nanotechnology Group, Central Electronics Engineering Research Institute (Council of Scientific and Industrial Research), Pilani-333031, India;* [c]*Department of Physics, Bangalore University, Bangalore-560056, India*

(*Received 5 May 2010; final version received 7 January 2011*)

$Ni/SiO_2/Si$ MOS structures were fabricated on n-type Si wafers and were irradiated with 50 MeV Li^{3+} ions with fluences ranging from 1×10^{10} to 1×10^{12} ions/cm^2. High frequency C–V characteristics are studied *in situ* to estimate the build-up of fixed and oxide charges. The nature of the charge build-up with ion fluence is analyzed. Defect levels in bulk Si and its properties such as activation energy, capture cross-section, trap concentration and carrier lifetimes are studied using deep-level transient spectroscopy. Electron traps with energies ranging from 0.069 to 0.523 eV are observed in Li ion-irradiated devices. The dependence of series resistance, substrate doping and accumulation capacitance on Li ion fluence are clearly explained. The study of dielectric properties ($\tan\delta$ and quality factor) confirms the degradation of the oxide layer to a greater extent due to ion irradiation.

Keywords: DLTS; MOS; ion irradiation; deep-level traps; oxide charges; dielectric loss

1. Introduction

The existence of strong radiation in cosmic environments is well known, and its effects on semiconductor devices have been continuously studied for over four decades. MOS (metal–oxide–semiconductor) devices are practically a base part of all electronic circuits and are extensively used in space applications because of their fast switching speeds and simple drive requirements. However, these devices are very sensitive to radiation exposure and are prone to parametric changes or even functional failure. The modification of electrical characteristics of MOS structures induced by radiation damage is determined by a combined structural response of the oxide and semiconductor layers. These layers, being the main composite of MOS structures, are known to have different sensitivities to ionizing radiation, especially at high electronic stopping powers. Considerable data have been already acquired that give information about the defects induced by γ/X-rays, electron or proton irradiation in Si–SiO_2 structures. The interaction of such radiation with the target is dominated by electronic energy loss. As far as ion

*Corresponding author. Emails: nshash@gmail.com; ku_shashank@rediffmail.com

ISSN 1042-0150 print/ISSN 1029-4953 online
© 2011 Taylor & Francis
DOI: 10.1080/10420150.2011.553954
http://www.informaworld.com

irradiation is concerned, low-energy particles mainly transfer their kinetic energies onto the target nuclei (nuclear stopping), resulting in the creation of vacancy–interstitial pairs. In the high-energy range, the incident ion collides with the target electrons and thus inducts in its trail a high density of ionized target atoms (electronic stopping). The energy deposited on electrons is transferred to the atoms, causing permanent damage in oxides.

The study of the defect generation process in MOS devices continues to unveil new and interesting physical phenomena. Heavy ions in space can degrade the oxides in electronic devices through several different mechanisms, and a satisfactory understanding and explanation of the experimental results has not yet been accomplished. Therefore, the study of swift heavy ion irradiation in electronic materials and devices is still a subject of fundamental and technological significance (*1–9*).

In the present work, the $Ni/SiO_2/Si$ MOS structures were irradiated with high-energy Li ions as they represent a promising alternative radiation source for radiation hardness studies (*10, 11*). *In situ* high-frequency $C–V$ measurement was performed for various fluences of Li ions in order to precisely estimate the variation of trap densities in the oxide. A more recent and widely used technique, deep-level transient spectroscopy (DLTS), was used to characterize the deep levels in the silicon band gap, as it overcomes the drawbacks of other conventional techniques such as thermally stimulated current and thermally stimulated capacitance measurements in view of its better immunity to noise and surface channel leakage current. DLTS is a sensitive tool and detects the trap concentrations as low as 10^{-4} in order. It exhibits a peak for each trap generated and allows obtaining parameters from either minority carrier traps (positive peak in the spectrum) or majority carrier traps (negative peak). DLTS is a useful tool for defect analysis (*12*) as it offers easy and direct interpretation of experimental results.

Downloaded By: [CSIR eJournals Consortium] At: 05:32 27 March 2011

2. Materials and methods

The MOS structures were prepared in clean room facilities at the Central Electronics Engineering Research Institute (CEERI), Pilani, India. Structures were based on a silicon wafer: ⟨100⟩ oriented, n-type, phosphorous doped, 1.5 inch diameter and 220 μm thick. The sheet resistance was measured to be 20–22 Ω/square. Standard cleaning procedures such as RCA-I, RCA-II and piranha were carried out as part of the wafer-cleaning process. The wafer was loaded into the oxidation furnace at 800 °C in N_2 ambient. The thermal oxide growth was conducted at 1050 °C in a dry oxygen atmosphere for 22 min. The wafer was cooled at a rate of ∼1 °C/s in N_2 ambient and unloaded from the furnace at 800 °C. The oxide thickness measured using an ellipsometer is found to be 72 nm. Metallization of the gate was done under vacuum of 10^{-7} torr using Varian's e-beam metallization unit. Circular Ni dots of 2 mm diameter were photo-lithographically defined. Silver was used to provide ohmic contact on the backside of the wafer.

The MOS structures were irradiated with swift 50 MeV Li^{3+} ions using the 15 UD 16 MV Pelletron Tandem Van De Graff Accelerator facilities at Inter-University Accelerator Centre (IUAC), New Delhi. The MOS capacitors were ground and irradiated from the gate side for different fluences ranging from 1×10^{10} to 1×10^{12} ions/cm^2. The ion fluences were calculated by measuring the ion current and irradiation time. The ion beam current was fixed at 1 pnA. During irradiation, the target chamber was maintained at room temperature (300 K) and low pressure (∼10^{-9} torr). The range of 50 MeV Li ions in silicon was calculated to be about 310 μm using SRIM (stopping power and range of ions in matter) tools.

For *in situ* measurements, the samples were mounted on a ladder in a UHV irradiation chamber from which electrical connections were brought out to the control room. *In situ* $C–V$ measurements at 1 MHz AC frequency were recorded subsequent to each irradiation fluence of Li^{3+} ions using the BOONTON 7200 $C–V$ measurement system. Trap densities of fixed charges and oxide charges

were determined using the C–V curves. DLTS spectra were recorded for both the unirradiated MOS capacitor and three different MOS capacitors (diced from the same processed wafer) exposed to Li ions at three different fluences. The trap concentration, activation energy and capture cross-section of different deep levels were determined by DLTS spectra. The DLTS system (IMS-2000) employed for the present study consisted of a boxcar averager, a pulse generator, a thousand point digitizer, a voltage generator and a high-speed capacitance meter. The pulse generator is capable of generating pulses with widths ranging from 100 ns to 10 s. The pulse height could be programmed from −12 V to +12 V. The boxcar averager is capable of generating seven rate windows. The time constants can be varied from 1 ms to 2 s. In the present study, DLTS spectra were recorded with a reverse bias of 5 V and pulse width of 20 ms applied between the gate and the substrate.

Downloaded By: [CSIR eJournals Consortium] At: 05:32 27 March 2011

3. Experimental results and discussion

3.1. In situ *high-frequency C–V analysis*

C–V measurements at 1 MHz frequency were carried out *in situ* for various lithium ion fluences ranging from 1×10^{10} to 1×10^{12} ions/cm^2. A negative shift in the C–V curves (Figure 1) clearly indicates the build-up of positive charges in the oxide due to ion irradiation (*4, 13*). From the C–V curves, the change in the flat band voltage (V_{FB}) for various fluences of Li ions was measured by calculating the flat band capacitance (C_{FB}). The normalized flat band capacitance was calculated to be 0.85 using the equation

$$\frac{C_{FB}}{C_{OX}} = \frac{1}{1 + \left((136\sqrt{T/300})/W_{OX}\sqrt{N_D}\right)}, \quad (1)$$

where C_{OX} is the oxide capacitance, T is the temperature (K), W_{OX} is the oxide thickness and N_D is the donor doping concentration (cm^{-3}).

The fixed charge density (N_F) of the device exposed to various fluences of Li ions was calculated using the equation

$$N_F = \frac{(\varphi_{ms} - V_{FB})\, C_{OX}}{q}, \quad (2)$$

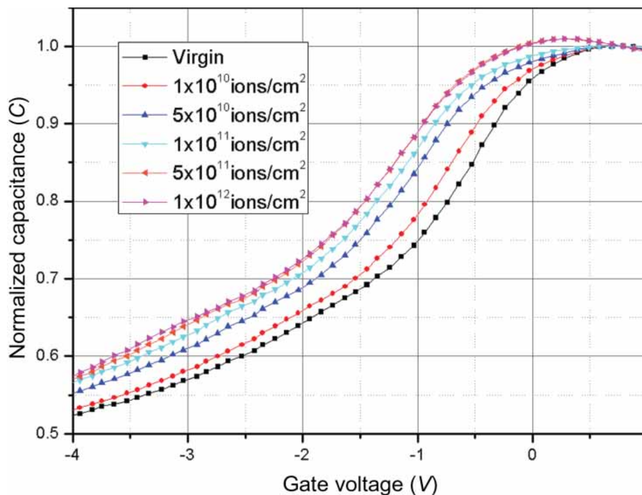

Figure 1. C–V curves at 1 MHz ac frequency before and after Li ion irradiation.

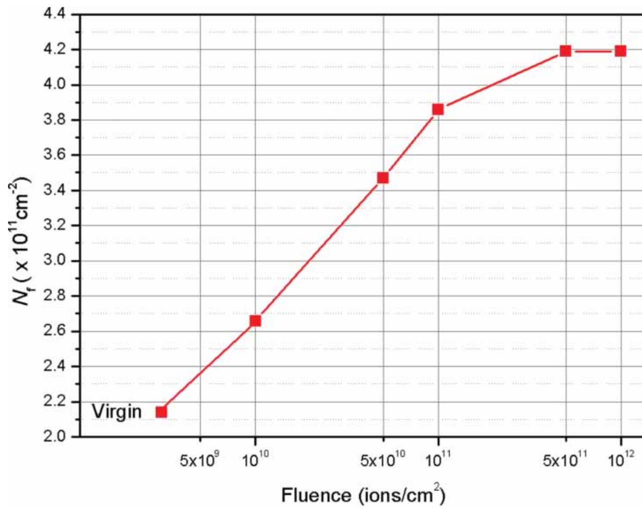

Figure 2. Fixed charge densities of virgin and Li ion-irradiated MOS capacitors.

Downloaded By: [CSIR eJournals Consortium] At: 05:32 27 March 2011

where q is the elementary charge. The metal–semiconductor work function (φ_{ms}) was calculated to be 0.2 V (*14*). The fixed charge density increases from 2.1×10^{11} cm^{-2} for the virgin device to about 4.2×10^{11} cm^{-2} for a Li fluence of 1×10^{12} ions/cm^2 as shown in Figure 2. The build-up of oxide charges due to ion irradiation was calculated using Equation (3) and is shown in Figure 3.

$$N_{OX} = \frac{-\Delta V_{FB} C_{OX}}{q}. \tag{3}$$

The oxide charge density is found to increase from 1.5×10^{11} cm^{-2} (for the virgin device) to 3.9×10^{11} cm^{-2} for a Li fluence of 1×10^{12} ions/cm^2. The build-up of fixed and oxide charge densities both exhibit a parabolic behavior, where the build-up tends to saturate after a certain level of ion irradiation (which is 5×10^{11} ions/cm^2 in the present case). Another important observation in the normalized capacitance curves (Figure 1) is the small increase in the depletion and

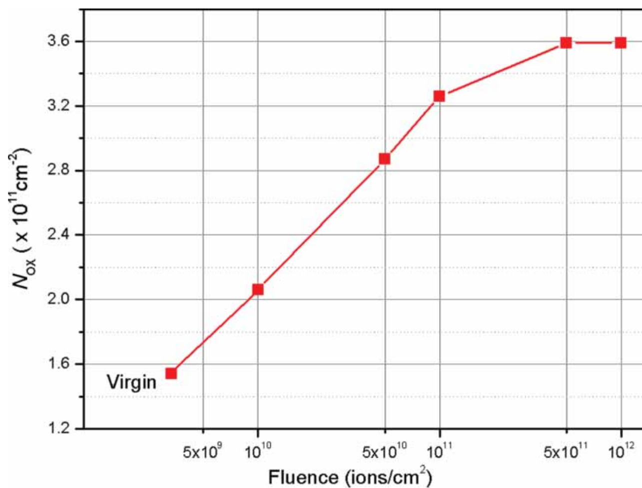

Figure 3. Oxide charge densities of virgin and Li ion-irradiated MOS capacitors.

inversion capacitance with the increase in ion fluence. Even though the curves show an increasing capacitance with the fluence for a negative gate voltage, the curves actually start merging at positive potential. Further, for a gate voltage more than +1 V, the capacitance decreases with the fluence. The offline capacitance measurements made at a gate voltage of +5 V after 12 h of irradiation also shows a decreasing capacitance with increasing fluence.

3.2. *DLTS measurements*

In principle, ion irradiation can damage the semiconductor devices by two mechanisms: ionization and displacement. While ionization damage creates electron–hole pairs, displacement damage results in the generation of several types of defects such as vacancy, interstitial, di-vacancy, Frenkel pair, and vacancy–impurity complexes, namely A-center (V–O), E-center (V–P), boron–carbon interstitial clusters and di-interstitial or higher-order complexes called D-centers (*15*).

The deep-level defects generated by irradiation were characterized by the DLTS technique. The DLTS spectrum is a plot of the difference in capacitance (δC) versus temperature. Figure 4 exhibits the DLTS spectra of Li^{3+} ion-irradiated MOS capacitors for three different ion fluences. The trap concentration (N_T) can be determined by knowing the peak height (δC_{max}) in the DLTS spectrum. Activation energy (ΔE) and capture cross-section (σ) of the deep levels are calculated

Downloaded By: [CSIR eJournals Consortium] At: 05:32 27 March 2011

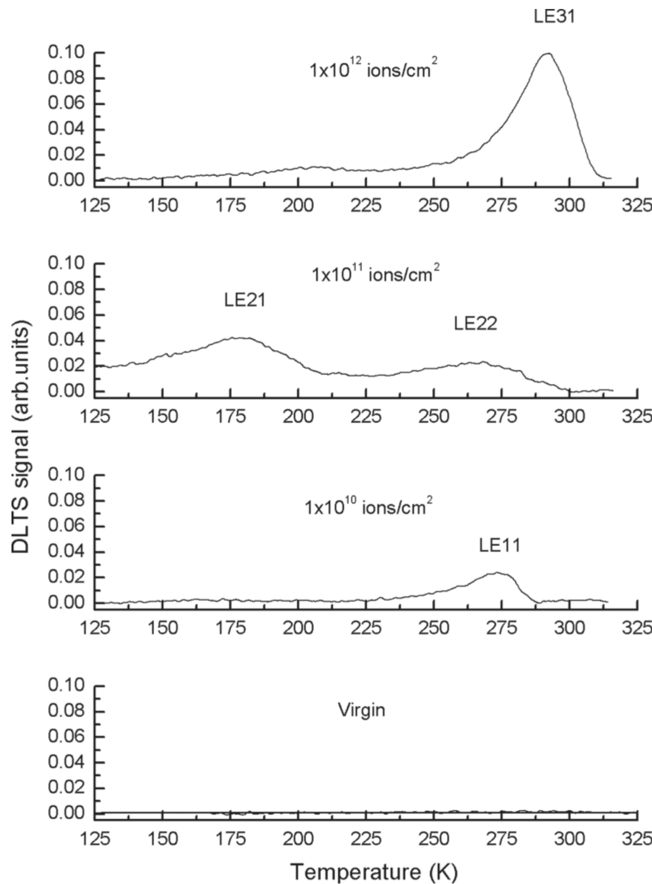

Figure 4. DLTS spectrum of virgin and Li ion-irradiated devices.

by using the equation

$$\tau T^2 = \frac{\exp[(\Delta E)/kT]}{\gamma\sigma}. \tag{4}$$

In this equation, γ is the material coefficient, T the temperature and τ the time constant. A plot of $\ln(\tau T^2)$ versus $1/T$ is known as the Arrhenius plot; the activation energy of the deep level defect ΔE is obtained from the slope of the plot and the capture cross-section is obtained by extrapolating the plot on the Y-axis. Figures 5–7 exhibit the Arrhenius plots of deep level defects for three different ion fluences. Only one majority carrier deep level defect is observed in the DLTS spectra of the Li^{3+} ion-irradiated MOS capacitor with an ion fluence of 1×10^{10} ions/cm^2 and 1×10^{12} ions/cm^2. For the ion fluence of 1×10^{11} ions/cm^2, two majority carrier defect levels are observed. The trap concentration, capture cross-section and introduction rate of all the

Downloaded By: [CSIR eJournals Consortium] At: 05:32 27 March 2011

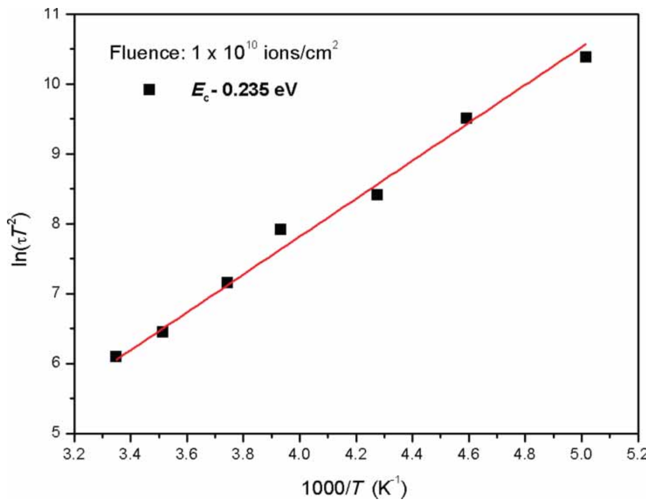

Figure 5. Arrhenius plot for the Li ion fluence of 1×10^{10} ions/cm^2.

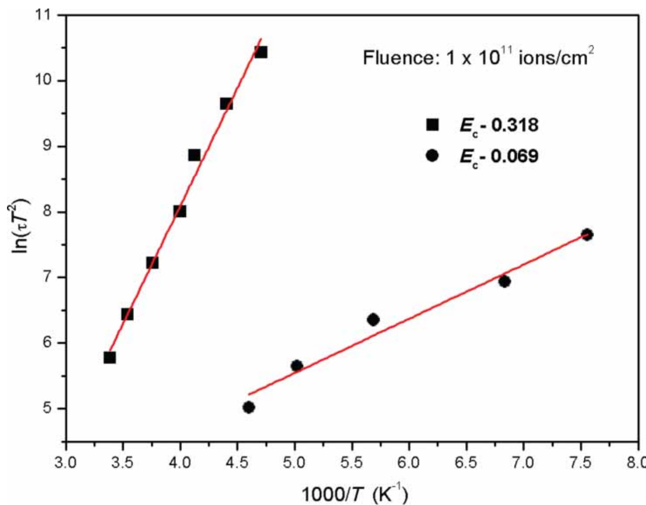

Figure 6. Arrhenius plots for the Li ion fluence of 1×10^{11} ions/cm^2.

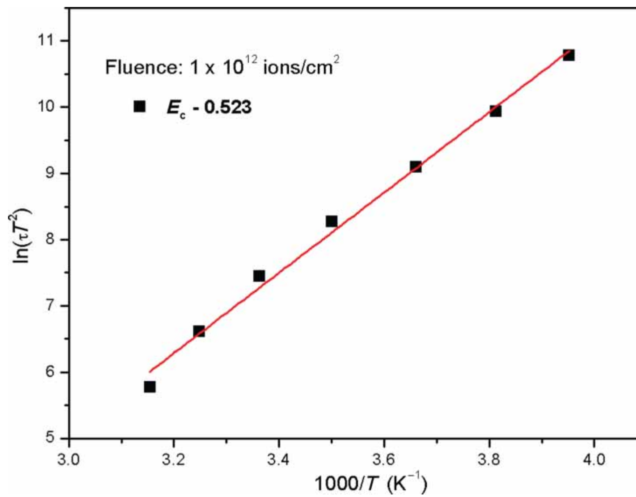

Figure 7. Arrhenius plots for the Li ion fluence of 1×10^{12} ions/cm^2.

Downloaded By: [CSIR eJournals Consortium] At: 05:32 27 March 2011

deep level defects are calculated from the DLTS spectra and are presented in Table 1. In Table 1, "Trap concentration" represents the trap density of a particular defect type while, "Total trap concentration" represents the total trap density of all defect types for a particular fluence of Li ion irradiation.The activation energy of all the defects has been measured to an accuracy of 0.001 eV.

The recombination of electron–hole pairs at the defect levels generated by the high-energy ions is dependent on the trap concentration. The recombination lifetime is calculated using the following equation and is tabulated in Table 1:

$$\tau = \frac{1}{\sigma_n v_{th} N_T}. \quad (5)$$

In Equation (5), σ_n is the minority carrier capture cross-section, v_{th} is the thermal velocity of the carriers and N_T is the total trap concentration. The values of the effective recombination lifetime and total trap concentration of the observed deep level defects are also presented in Table 1. The deep level defects in silicon have been studied by many research groups (*16–18*), and the identification of the defect type is made on the basis of the activation energy and capture cross-section and a comparison with those reported in the literature.

The E in the defect label symbolizes an electron trap. The defect energy level E11 with an activation energy of E_c – 0.235 eV is observed for the device irradiated with lithium ions at a fluence 1×10^{10} ions/cm^2. This defect is attributed to a di-vacancy (*19–22*) and acts as a good generation–recombination (G–R) center, which can be the source of leakage currents (*23*). A di-vacancy is the defect formed by two adjacent vacancies. Two defect levels, labeled E21 and E22, are found in the device irradiated with an ion fluence of 1×10^{11} ions/cm^2. The activation energies of these levels are E_c – 0.069 eV and E_c – 0.318 eV, respectively. The energy level E_c – 0.069 eV is attributed to the Si self-interstitial (*24*), which acts as a good recombination center. The defect level E_c – 0.318 eV is found to be an A-center (V–O) (19). The defect labeled E31 with energy E_c – 0.523 eV is a new type of defect found in n-type devices when irradiated with an ion fluence of 1×10^{12} ions/cm^2. This defect level can probably be attributed to higher-order complexes, a D-center, as referenced by the nearest energy level reported in the literature (*25*). In the DLTS spectrum, the peak height represents the trap concentration. The concentration of the defects is found to increase from 2.26×10^{15} to 5.04×10^{15} cm^{-3} for a total ion fluence of 1×10^{12} ions/cm^2, as shown in Table 1. It can also be observed from Table 1 that the effective

Downloaded By: [CSIR eJournals Consortium] At: 05:32 27 March 2011

Table 1. Data obtained from the analysis of DLTS spectra for Li-irradiated MOS capacitors.

Ion fluence (ions/cm^2)	Defect label	Defect type	Activation energy (eV)	Trap concentration (cm^{-3})	Total trap concentration (cm^{-3})	Capture cross-section (cm^2)	Introduction rate (cm^{-1})	Recombination lifetime (s)	Effective lifetime (s)
1×10^{10}	E11	Di-vacancy	$E_c - 0.235$	2.26×10^{15}	2.26×10^{15}	1.15×10^{-20}	226.0×10^3	3.68×10^{-3}	3.68×10^{-3}
1×10^{11}	E21	Si(i)	$E_c - 0.069$	2.66×10^{15}	3.42×10^{15}	1.09×10^{-22}	266.8×10^3	4.36×10^{-1}	2.90×10^{-4}
	E22	A-center (V–O)	$E_c - 0.318$	7.60×10^{14}		4.43×10^{-19}	7.602×10^3	2.90×10^{-4}	
1×10^{12}	E31	D-center	$E_c - 0.523$	5.04×10^{15}	5.04×10^{15}	2.79×10^{-16}	5.046×10^3	6.37×10^{-8}	6.37×10^{-8}

Table 2. Data obtained from offline C–V measurements using phase impedance analyzer.

Li ion fluence (ions/cm^2)	Series resistance (Ω)	Capacitance (pF)	tan δ	Quality factor	Substrate doping (cm^{-3})
5×10^{10}	8.1456	789.64	0.039609	25.247	4.53×10^{16}
1×10^{11}	8.2401	777.81	0.040114	24.929	3.82×10^{16}
5×10^{11}	14.736	731.64	0.066937	15.064	2.84×10^{16}
1×10^{12}	28.039	623.19	0.10431	9.5873	1.59×10^{16}

carrier lifetime decreases from 3.68×10^{-3} to 6.37×10^{-8} s due to Li ion irradiation of MOS devices.

3.3. *Effects on dielectric properties*

Downloaded By: [CSIR eJournals Consortium] At: 05:32 27 March 2011

Off-line capacitance measurements were carried out using a phase impedance analyzer in order to study the series resistance, substrate doping and dielectric properties of the device. All the said parameters were extracted at 1 MHz AC frequency. The doping concentration is calculated by plotting $1/C^2$ versus gate voltage, and it can be observed from the Table 2 that the doping concentration reduces as a function of fluence. The reduction in doping concentration is mainly because of the strained bonds associated with majority carriers trapped in radiation-induced deep levels (*11*). This dopant reduction effect indeed causes the series resistance to increase and in turn causes the capacitance to decrease (*26, 27*).

In the present measurements, the dielectric loss tangent (tan δ) extracted from capacitance measurements is found to increase as the ion fluence increases. The dielectric loss tangent (tan δ) is related to dielectric constant by the equation:

$$\tan\delta = \frac{4\pi\sigma_{\mathrm{dc}}}{\omega\varepsilon'}, \qquad (6)$$

where σ_{dc} is the dc conductivity, ω the frequency and ε' is the real part of the dielectric constant given by the product of $\varepsilon^0 * \varepsilon^r$ (*8*). The increase in tan δ is attributed to the decrease in the dielectric constant of the oxide with ion fluence (*28*). From the offline C–V measurements, the dielectric constant was found to reduce from ~2.4 (for the device irradiated with 5×10^{10} Li ions/cm^2) to 1.8 (for the device irradiated with 1×10^{12} Li ions/cm^2). It can also be observed from Table 2 that the quality factor ($1/\tan\delta$) of the dielectric is reduced from ~30 to 9.5 for a total Li dose of 1×10^{12} ions/cm^2. This clearly indicates that Li ion irradiation degrades the quality of the oxide to a greater extent giving rise to a decreased capacitance.

4. Conclusion

The negative shift in the high-frequency C–V characteristics of Ni/SiO_2/Si MOS capacitor structures when irradiated with 50 MeV Li^{3+} ions clearly indicates the build-up of positive charges in the oxide. The *in situ* C–V measurement shows that the charge build-up is parabolic in nature and tends to saturate at a Li fluence of 5×10^{11} ions/cm^2. Deep level defects introduced in the silicon band gap are identified as electron traps whose activation energies range from $E_c - 0.069$ to $E_c - 0.523$ eV. The activation energy, capture cross-section and concentration of observed deep level defects are studied using the DLTS technique. The results indicate an increase in fixed charge and oxide charge densities and bulk trap concentration, with the decrease in the carrier lifetime due to the Li ion irradiation. The study of the dielectric properties reveals a degradation of the oxide, where the quality factor is reduced to almost one-third of its original value after ion irradiation.

Acknowledgements

The authors thank Mr G.S. Negi, CEERI, Pilani, for his support during the fabrication of devices. The authors are also grateful to Mr Saif A. Khan and Mr Sugam Kumar, IUAC, New Delhi, for their cooperation during the experiments conducted at IUAC.

References

(1) Stano, J.; Skuratov, V.A.; Ziska. M.; Kovac, P. *Vacuum* **2005,** *78,* 627–630.
(2) Srivastava, P.C.; Sinha, O.P.; Tripathi, J.K.; Kabiraj, D. *Semicond. Sci. Technol.* **2002,** *17,* L44–L46.
(3) Hughes, H.L.; Benedetto, J.M. *IEEE Trans. Nucl. Sci.* **2003,** *50* (3), 500–521.
(4) Schwank, J.R.; Fleetwood, Felix, J.A.; Dodd, P.E.; Paillet P.; Ferlet-Cavrois, V. *IEEE Trans. Nucl. Sci.* **2008,** *55* (4), 1833–1853.
(5) Lenahan, P.M.; Bohna, N.A.; Campbell, J.P. *IEEE Trans. Nucl. Sci.* **2002,** *49* (6), 2708–2712.
(6) Tataroglu, A.; Altındal, S.; Karadeniz, S.; Tugluoglu, N. *Microelectron. J.* **2003,** *34,* 1043–1049.
(7) Kim, H.S.; Hyun, J.W.; Noh, S.J. *Curr. Appl. Phys.* **2006,** *6,* 185–187.
(8) Tugluoglu, N.; Altindal, S.; Tataroglu, A.; Karadeniz, S. *Microelectron. J.* **2004,** *35,* 731–738.
(9) Kaschieva, S.; Gueorguiev, V.; Halova, E.; Dmitriev, S.N. *Bulg. J. Phys.* **2006,** *33,* 48–54.
(10) Candelori, A.; Bisello, D.; Giubilato, P.; Kaminski, A.; Litovchenko, A.; Lozano, M.; Ullan, M.; Rando, R.; Wyss, J. *Nucl. Instrum. Methods A* **2004,** *518* (1–2), 338–339.
(11) Candelori, A.; Bisello, D.; Dalla Betta, G.F.; Giubilato, P.; Kaminski, A.; Litovchenko, A.; Lozano, M.; Petrie, J.R.; Rando, R.; Ullan, M.; Wyss, J. *IEEE Trans. Nucl. Sci.* **2004,** *51* (5), 1–7.
(12) Garcia, A.A.; Reyes Barranca, M.A. *Rev. Mex. Fis*. **2002,** *48* (6), 539–547.
(13) Ma, T.P.; Dressendorfer, P.V: *Ionizing Radiation Effects in MOS Devices and Circuits;* John Wiley & Sons: New York, 1989.
(14) Sze, S.M. *Physics of Semiconductor Devices;* Wiley Inter-Science: New Jersey, 1981.
(15) Madhu, K.V.; Kulkarni, S.R.; Ravindra, M.; Damle, R. *Semicond. Sci. Technol.* **2007,** *22,* 963–969.
(16) Vujicic, M.; Borjanovic, V.; Pivac, B. *Mat. Sci. Eng. B* **2000,** *71,* 92–95.
(17) Kaschieva, S.; Christova, K.; Dmitriev, S.N. *J. Optoelectron. Adv. Mater.* **2009,** *11* (10), 1494–1497.
(18) Shinoda, K.; Ohta, E. *Appl. Phys. Lett.* **1992,** *61,* 2691–2693.
(19) Madhu, K.V.; Kulkarni, S.R.; Ravindra, M.; Damle, R. *Nucl. Instrum. Methods B* **2007,** *254,* 98–104.
(20) Madhu, K.V.; Ravi Kumar; Ravindra, M.; Damle, R. *Solid-State Electron.* **2008,** *52,* 1237–1243.
(21) Pellegrino, P.; Leveque, P.; Lalita, J.; Hallen, A.; Jagadish, C.; Svensson, B.G. *Phys. Rev. B* **2001,** *64,* 195211-1–9.
(22) Kaschieva, S.; Gueorguiev, V.; Halova, E.; Dmitriev, S.N.; *Bulg. J. Phys.* **2006,** *33,* 48–54.
(23) Kang, I.-M.; Kwon, H.-I.; Myung Won Lee; Park, B.-G.; Lee, J.D.; Park, S.S.; Ahn, J.C.; Lee, Y.H. *J. Korean Phys. Soc.* **2004,** *44,* 69–72.
(24) Lafevre, H. *Appl. Phys. A* **1982,** *29,* 105–111.
(25) Madhu, K.V.; Kulkarni, S.R.; Ravindra M.; Damle, R. *Radiat. Eff. Def. Solids* **2008,** *163* (11), 873–883.
(26) Sahin, B.; Cetin, H.; Ayyildiz, E. *Solid State Commun.* **2005,** *135,* 490–495.
(27) Vikram Singh; N. Shashank, N.; Dinesh Kumar; Nahar, R.K. *Radiat. Eff. Def. Solids* **2011,** *166* (2), 80–88.
(28) Thangadurai, P.; Kaplan, W.D.; Mikhelashvili, V.; Eisenstien, G. *Microelctron. Reliab.* **2009**, *49,* 716–720.

Downloaded By: [CSIR eJournals Consortium] At: 05:32 27 March 2011